# Templating rare-earth hybridization via ultrahigh vacuum annealing of $ErCl_3$ nanowires inside carbon nanotubes

Paola Ayala,[1] Ryo Kitaura,[2] Ryo Nakanishi,[2] Hidetsugu Shiozawa,[3] Daisuke Ogawa,[2] Patrick Hoffmann,[4] Hinsanori Shinohara,[2] and Thomas Pichler[1]

[1]*University of Vienna, Faculty of Physics, 1090 Vienna, Austria*

[2]*Department of Chemistry, Nagoya University, Nagoya 464-8602, Japan*

[3]*Advanced Technology Institute, University of Surrey, Guildford GU2 7XH, United Kingdom*

[4]*BESSY II, D-12489 Berlin, Germany*

(Received 12 August 2010; revised manuscript received 10 December 2010; published 11 February 2011)

Here we report on controlling the effective hybridization and charge transfer of rare-earth elements inside a carbon nanotube (CNT) nanoreactor. The tubular space inside CNTs can encapsulate one-dimensional (1D) crystals such as $ErCl_3$, which we have used as a starting material. Applying a thermochemical reaction in ultrahigh vacuum, we obtain elemental Er nanowires still encapsulated in the CNTs. The hybridization degree and the effective charge changes were directly accessed across the Er 4*d* and 3*d* edges by high-energy spectroscopy. It was found that Er is trivalent but the effective valence is reduced for the Er-filled tube, which strongly suggests an increased hybridization between the nanotube $\pi$ states and the Er 5*d* orbitals. This was also evidenced by the conduction band response determined in C1*s*–x-ray absorption spectroscopy (XAS). These results have significant implications for the 1D electronic and magnetic properties of these and similar rare-earth nanowire hybrids.

DOI: 10.1103/PhysRevB.83.085407 PACS number(s): 73.63.Fg, 71.10.Hf, 71.20.Tx

## I. INTRODUCTION

The unique crystalline structures of single-walled carbon nanotubes (SWCNTs) have become a major object of technological and scientific interest, propelled to an unprecedented level by their own exceptional electronic and optical properties.[1] These one-dimensional (1D) conductors with unusual transport properties owe their mechanical and electronic behavior mainly to their internal arrangement of carbon atoms with $sp^2$ hybridization. A further range of functionalities can be imagined through the modification of the inner and outer wall of the nanotubes,[2] which is one of the main reasons why filling them with different materials has gained considerable attention in recent years, especially regarding synthesis routes.[3–12]

In this study we report on the electronic properties of a hybrid structure that encapsulates an $ErCl_3$ nanowire inside the hollow structure of a SWCNT. Within this still vast scientific field, these structures represent an ideal system for fully understanding dimensionally confined phenomena. Crystal structures such as lanthanide nitrides and chlorides were studied intensively in the 1960s and 1970s.[13–17] Although from a different scale approach, their crystallographic structure and phase transformations have been deeply examined and give rise to interesting optical and magnetic properties. The present work deals with the understanding of such properties together with the implied dimensionality. In a recent paper we have studied in detail the structure of crystalline $ErCl_3$ nanowires templated inside carbon nanotubes.[10] In particular, this method has been thought of as a feasible path to fabricate various low-dimensional metal complex nanowires and characterize their structural and magnetic properties, envisaging new fields in the science and technology of carbon nanotubes (CNTs) and related low-dimensional nanomaterials. The effective valence state of Er in the filled $ErCl_3$ nanowires was determined by 3*d* x-ray absorption spectroscopy (XAS) and Er was found to be $Er^{3+}$. However, no detailed information on the modification of the electronic structure could be retrieved.

In this paper we explore in detail the electronic structure of $ErCl_3$ nanowire-filled SWCNTs and their modification via high-temperature ultrahigh vacuum (UHV) annealing. A combination of resonant photoemission (RES-PES) and XAS is used as a versatile tool to provide information on the charge transfer and bonding environment in the filled material compared to the pristine nanotube templates. This allows us to evaluate the changes in the electronic structure of the valence and conduction band of the filled CNT hybrids. From XPS we observe a change in hybridization between the fillers and the nanotubes, which goes hand in hand with the decomposition of $ErCl_3$ and the formation of Er nanowires inside carbon nanotubes. The amount of hybridization and the effective charge state of Er was monitored by a combination of XAS and resonant (RES) PES across the Er 4*d* and 3*d* edge. In both compounds Er is trivalent, but the effective valence is reduced for the Er nanowire hybrid. This points toward an increased hybridization between the nanotube $\pi$ states and the Er 5*d* orbitals, which is also evidenced by the conduction band response determined in C1*s* XAS.

## II. EXPERIMENTAL

The synthesis method of the materials used here was reported in Ref. 9, which mainly involves tailoring under high temperature and vacuum. These quantum nanowires exhibit a very high filling ratio (∼90%).[10] The structure of crystalline $ErCl_3$ nanowires templated inside the hollow core of the SWCNTs has been done using direct injection pyrolytic synthesis (e-DIPS) (Ref. 18) with a subsequent nanotube opening in at 600 °C and later filling using anhydridous $ErCl_3$. The e-DIPS SWCNTs used here have a large diameter distribution (the average diameter is $1.9 \pm 0.96$ nm). It is

 

important to note that the crystal structure of the encapsulated $ErCl_3$ varies with the diameter of the hosting SWCNT.

For XAS and PES spectroscopic studies, pristine samples without filling as well as the same material with encapsulated $ErCl_3$ nanowires were mounted on Mo sample holders. The pristine reference materials were purified SWCNTs with a narrow Gaussian diameter distribution. All the measurements are performed on a bulk agglomerate annealed above 800 K in ultrahigh vacuum. The XAS and RES-PES experiments here reported were performed at the beamline UE52PGM at BESSY II, which has a resolving power ($E/\Delta E$) of $1 \times 10^4$. The XAS spectra were recorded in partial yield and drain current modes. XPS line-shape analysis was also done for a detailed analysis of the chemical state and the bonding environment.

## III. RESULTS AND DISCUSSION

This study comprises two stages of the hybrid material. At first instance, we studied in detail the electronic properties of the $ErCl_3$-filled SWCNTs, in which a mild heat treatment was applied resistibly in order to eliminate the possible oxygen or atmospherical contaminants formed on air exposure between their production and the measurements. A second phase was applied with e-beam heating. Subsequently, in both cases, the sample stoichiometry and purity were checked by a PES survey scan up to 1200 eV (not shown here). No contamination from oxygen or catalyst particles was detected in any sample within an experimental limit of 0.5% in these cases. From the relative change in the intensity ratio between the Er 4*d* and the C1*s* line, we can estimate the relative filling ratio in the $ErCl_3$ nanowire-filled sample and in the annealed sample. In the annealed sample about 1/3 of the Er is left.

To understand the electronic properties of the filled nanotubes as grown, as well as post e-beam heat treatment, it is particularly interesting to start from the carbon site in these new hybrid compounds. First, a closer insight to the C1*s* line shape recorded in photoemission with a photon excitation energy of 400 eV is shown in Fig. 1. From the bottom to the top, the signals corresponding to a reference sample (i.e., raw SWCNT material without filling), the $ErCl_3$ filled nanotubes, and the same filled hybrid material after heat treatment are depicted. We can observe clear evidence for a filling-induced downshift of the C1*s* binding energy (BE). In the case of the hybrid material without any heat treatment, an additional clear broadening of about 0.2 eV at the full width at half maximum (FWHM) is observed. This suggests a finite hybridization of the $ErCl_3$ states with the SWCNT, given that the shape of the C1*s* core level response in PES is related to the final state effects of the valence and conduction electrons. For pristine SWCNTs, the linewidth at the FWHM has a characteristic value of 0.26 eV, which is in very good agreement with previous high resolution photoemission reports made on metallicity mixed[19] and metallicity sorted[20] SWCNT samples. However, the shapes of the C1*s* line upon filling, and even more after heat treatment, exhibit obvious differences. In the case of the filled sample, a shoulder appears at lower binding energies (at 284.2 eV), which smears out in the sample with heat treatment (see Fig. 1). This shoulder can be assigned to a hybrid state between the $ErCl_3$ filling and the SWCNT $\pi$ orbitals. Additionally, the shift to lower binding energies observed in the middle spectrum backs away to a higher BE (slightly lower than the position for the pristine samples), which suggests a dehybridization of the nanotube wall and the filling upon the possible formation of clusters inside the SWCNTs. In order to better understand this, we have carried out a wide scan containing the primary strong signal for the C 1*s*, Er 4*d*, Cl 2*s*, and Cl 2*p* levels. The spectra recorded for the filled material before and after heat treatment are shown in the right panel of Fig. 1. In these XPS spectra it is evident that after heat treatment we find a decomposition of the $ErCl_3$ and a loss of the Cl atoms. This explains to a certain extent the broadening of the C1*s* line in the nonheated spectrum, and the narrower line shape in the sample upon thermal treatment, which can be attributed to changes in the degree of hybridization to nanotube carbon electronic states due to the transformation of the chemical composition of filling. Furthermore, the C1*s* PES spectra confirm to a first stage the possible formation of Er nanoclusters inside the SWCNT.

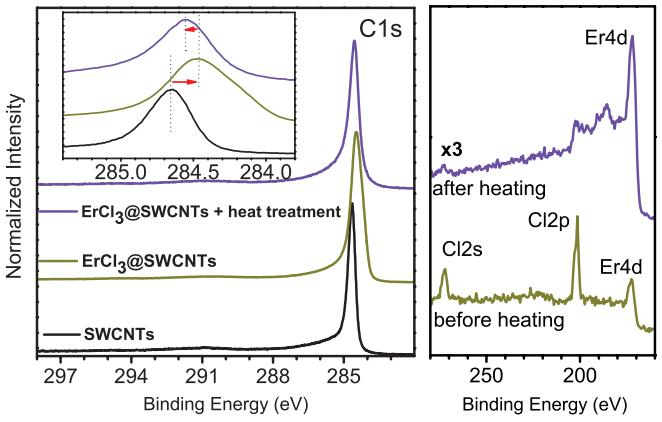


FIG. 1. (Color online) Photoemission spectra of the core level carbon C1*s* response for the reference (hollow SWCNTs) and filled $ErCl_3$@SWCNTs as produced and after thermal e-beam heating. Top right: XPS wide scan spectra showing the Er 4*d* and Cl primary responses together. The lower and upper lines correspond to the as-grown $ErCl_3$@SWCNTs as well as the material after heat treatment.

This explanation is further supported by XAS results. At the carbon site the XAS response is dominated by a broad $\pi^\star$ and $\sigma^\star$ response. The fine structure in the $\pi^\star$ response can be unambiguously assigned to the matrix element weighted density of states (DOS), which is strongly influenced by core hole effects along the tube axes and only weakly modified for the response from the van Hove singularities (vHs) polarized perpendicular to the tube axis.[19–22] The results of the C1*s* XAS response for the pristine and heat treated samples are depicted in Fig. 2 together with a line-shape analysis that includes the corresponding vHs (identified by the labels on top of the curves). This is in very good agreement with the results published previously for SWCNTs,[19–22] which clearly show the localized response from the vHs. In addition the foot at low energy can be assigned to the vHs of the semiconducting tubes, which is screened by the encapsulated material, as extensively discussed in Ref. 12. These screened vHs are labeled by $S_1^{M*}$ and $S_2^{M*}$. This corresponding foot is increased upon heat treatment and it can be assigned to an additional charge transfer

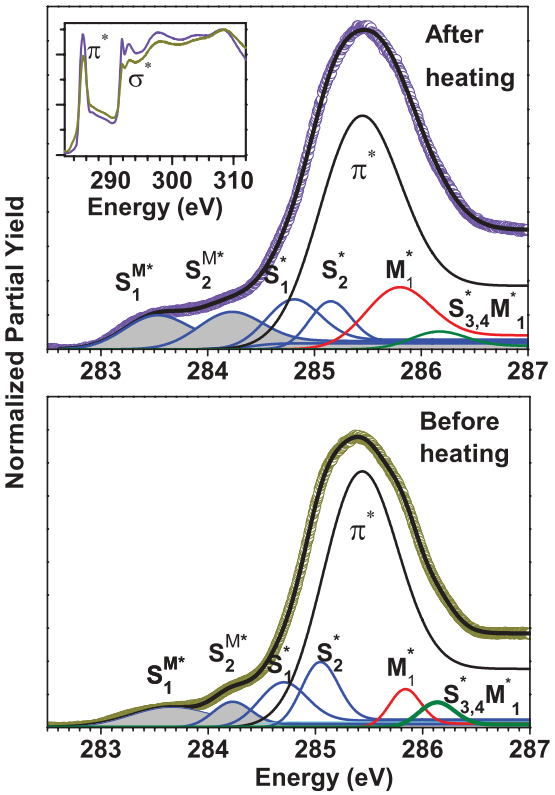


FIG. 2. (Color online) C1*s* absorption edges in x-ray absorption of filled $ErCl_3$@SWCNTs as produced and after e-beam heating. The inset on top shows the overall C1*s* edge and the main panels are a closeup into the $\pi^*$ resonance in which a foot appears at the lower energy region, which intensity increases on the sample after heat treatment. The recorded absorption edges (circles) of the $ErCl_3$@SWCNTs, after and before thermal treatment in vacuum, are depicted together with the results of a fitting and line-shape analysis that includes the labels denoting the van Hove singularities (vHs) and the overall conduction band $\pi^*$. The foot was fitted with the curves with shaded area, corresponding to the screened vHs in the conduction band: $S_1^{M*}$ and $S_2^{M*}$.

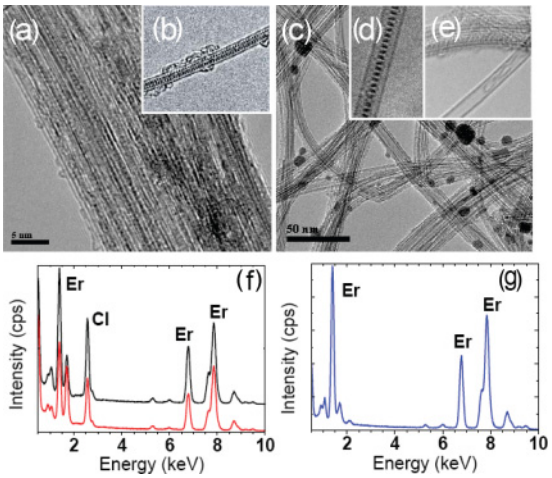


FIG. 3. (Color online) TEM micrograph of a SWCNT bundle filled with $ErCl_3$ (a) with an inset (b) corresponding to a high resolution TEM image of an individual $ErCl_3$-filled nanotube. In (c) appears the overall morphology of the filled NT material after heat treatment at 1000 K with insets (d) and (e) showing an individual tube where partial filling remains. The EDX spectra in the lower panels correspond to the material as synthesized [top spectrum in (f)], after resistive [lower spectrum in (f)], and e-beam heat treatment (g). The agglomerates in (c) have been inspected by EDX and they have been identified as elemental nanoparticles.

between the $ErCl_3$ and the C $\pi^*$. These results are concomitant to the observed change of hybridization observed in PES, as highlighted by the thermally induced vanishing of the shoulder at 284.2 eV in C1*s* PES, which is related to high hybridization of the erbium 5*d* orbitals with the carbon $\pi$ orbitals. The modifications at the Er site in the XAS of the Er 4*d* and 3*d* response are discussed later on.

To further analyze the possible formation of encapsulated nanoclusters, we performed an overall TEM bright field study at low and high magnifications, as well as additional energy dispersive x-ray (EDX) characterization. A global structural inspection is shown in Fig. 3. The intermediate and high magnification micrographs in Figs. 3(a) and 3(b) show the $ErCl_3$@SWCNTs hybrid material, which exhibits a very high filling ratio. The EDX spectrum recorded on a bundle of this material is shown on the black (top) spectrum depicted in Fig. 3(f). Although a full characterization was shown in Ref. 10, it is worth keeping in mind the very homogeneous filling and crystallinity of the initial filled nanotubes. The red (lower) spectrum depicted in Fig. 3 shows the Er and Cl signals in the EDX spectrum of a sample heated resistively. A slight decrease in intensity of the Cl signal in comparison to Er is seen. Additionally, we have analyzed the situation after heating of the $ErCl_3$@SWCNTs in a furnace and via e-beam heating in vacuum for 4 h. In both cases, the Cl atoms loss has been detected by EDX [a sample spectrum is shown in Fig. 3(g)]. This confirms the results obtained with XPS shown on the right panel spectra in Fig. 1, which suggest the release of Cl leading to the formation of elemental Er nanoclusters inside the nanotubes.

In any case, once the decomposition of $ErCl_3$ happens, the detection of atomic Er spectral features seems to be independent of the material location. Crystal field splitting is rather small for the lanthanides and is less important than spin-orbit coupling in regard to energy levels. For that reason, the outer diffusion of the Er clusters should not affect the next step in this study. We now turn to a further analysis of the hybridization state and bonding environment of the elements in the $ErCl_3$ nanowires at the Er site. For this purpose we have carried out an XAS and resonance photoemission combined study at the 4*d* and 3*d* resonances, respectively. With this, direct information can be obtained regarding the valence state of the encapsulated material, the degree of hybridization between the electronic states of the endohedral entity and the nanotube wall, and the charge transfer between the host and guest.

We have recorded the XAS spectra in the Er 3*d* and Er 4*d* levels shown in the left panels of Figs. 4 and 5, respectively. The right side corresponding figures depict the photoemission profiles in the valence band for the high resonance peaks arising in the XAS spectra, as well as off-resonance regions (these are pointed out with arrows in

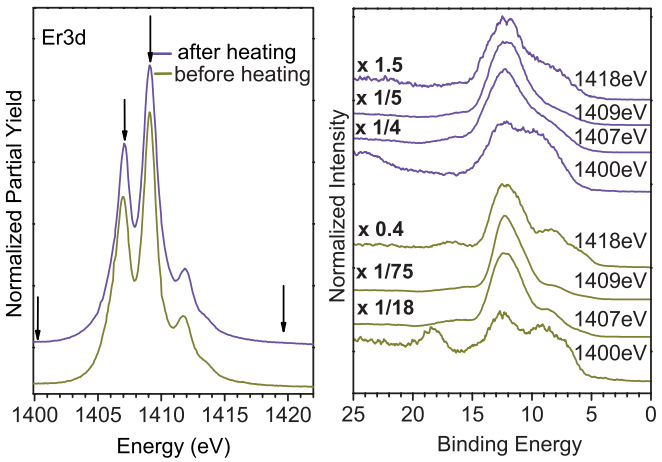


FIG. 4. (Color online) XAS response in the 3*d* levels of erbium (left) with the corresponding RES-PES study (right) of the valence band of the $ErCl_3$@SWCNTs, pre- and postheat treatment. Note that the arrows indicate the energy values at which the RES-PES right-side spectra were recorded. The numbers point toward the scaling factor responsible for the resonance enhancement.

Figs. 4 and 5). The excitation energies were calibrated by the Fermi edge of clean Au films and the XAS response was normalized to their background absorbance. The spectra show the valence band reflecting the occupied electronic states of the $ErCl_3$@SWCNTs (olive green spectra corresponding to the material before heating), as well as the Er nanoclusters (violet spectra labeled as after heating). In this case they show the occupied 3*d* and 4*d* orbitals (for these energy values the photoionization cross sections Er 3*d* and 4*d* levels dominate). However, the changes in the electron density of the filling material are affected by the hybridization with the 5*d* levels, as explained later. Note that in both cases, there is no increase of the DOS at the Fermi level.

The Er 3*d* and 4*d* XAS fingerprints in the left panels of Figs. 4 and 5 include the 3*d* to 4*f* and the 4*d* to 4*f* multiplets.

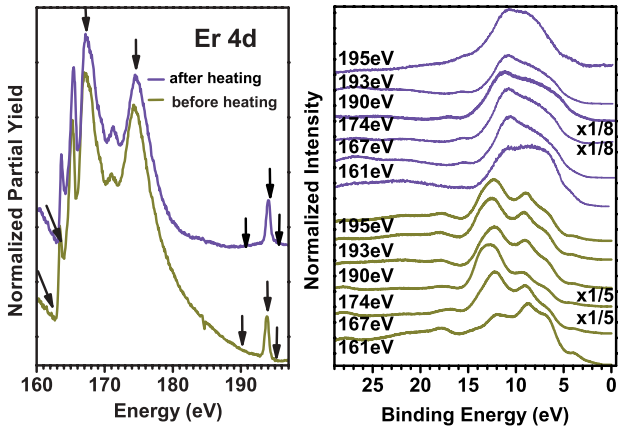


FIG. 5. (Color online) XAS response in the 4*d* levels of erbium (left) with the corresponding RES-PES study (right) of the valence band of the hybrid material. Note that the arrows indicate the energy values at which the RES-PES right-side spectra were recorded. The numbers point toward the scaling factor responsible for the resonance enhancement.

The spectral response is a direct fingerprint of the 4*f* count and in both cases the spectral shape is identical to the trivalent $Er^{III}$. In the case of $ErCl_3$, it can be safely assigned to ionic $Er^{3+}$, in good agreement with previous results.[10] Being a rare-earth metal, Er is characterized by an outer electronic structure comprised of localized 4*f* states that overlap the 5*d* and 6*s* orbitals. One of the effects of the localization of these states is a resonant absorption that occurs close to the core ionization threshold given the low BE of the 4*f* level.[23] For this reason, we have performed a detailed analysis in the resonance photoemission spectra. Here, the intensities recorded for the valence band of the material before and after thermal treatment provide direct information of the structural composition of the filling. Let us focus now primarily on the right side panel of Fig. 4, where the RES-PES study of the material in the pre- and postheat treatment conditions is depicted. In other words, we inspect more closely the RES-PES spectra across the 3*d* edge. The spectra are normalized to the ring current and the scaling factor labels indicate the spectra intensity in comparison to the intensity of the spectra recorded using 1400 eV as photon excitation energy (the two sets are scaled independently).

On examining the preresonance spectrum at 1400 eV, which is the off-resonance region for both situations, we find that a small peak corresponds to the main multiplet, which is in good agreement with atomic multiplet calculations for a $4f^{11}$ multiplet[24] observed at around 12.5 eV in binding energy. We observe that in both valence bands recorded with 1400 eV excitation energy, there is a much richer fine structure than in the upper spectra, and this is attributed to interference effects with the valence band electrons of the hybrid structure as a whole.[23,25,26] The multiplet is in close match to atomic multiplet calculations for $Er^{III}$. In the 3*d* to 4*f* multiplets, the transition is more localized than for the excitation of the shallow 4*d* levels and, therefore, the final state effects from interference with the molecular orbitals do not apparently play a significant role in the valence band. As highlighted in Fig. 4, the maximum of the 4*f* multiplet at about 12.5 eV has the strongest resonance enhancement of a factor 75 for the pristine sample, which is strongly reduced to a factor of 5 for the heat treated sample. Taking into account that in the off-resonance response the ratio between the Er 4*f* multiplet and the SWCNT DOS is reduced by a factor of 3 after heat treatment, we observe that the resonance is reduced by a factor of 5. This points toward a different charge distribution between the $4f^{11}$ multiplet and the $5d^1$ orbitals in the $Er^{III}$ and an enhanced hybridization of the $Er^{III}$ and the SWCNT DOS. This also suggests a reduced charge transfer, in good agreement with the discussion of the results from the complementary C1*s* site in these hybrid compounds. Focusing on the off-resonance spectra (1400 eV), we find that the resonance enhancement of the Er 4*f* levels at the maximum of the 3*d* edge in the samples after heating is 0.3, whereas that in the sample before heating is 0.1. This means that at 1400 eV, the resonance is roughly 1/3, which is significantly smaller for the heat treated samples; that is, the resonance factor is smaller in the case of the $ErCl_3$ than in the case of the heat treated samples in which only Er is formed.

On the other hand, as extracted from the Er 4*d* edge shown in Fig. 5, the valency of Er gives the same trend at higher energy resolution but the actual interference of the

shallow 4*d* core levels with the valence band response makes a nonambiguous analysis much more complicated. The most relevant information that we can actually obtain analyzing the spectra in the right panel of Fig. 5 is related to the hybridization of these heterostructures. The reduced resonance enhancement comparing the spectra before and after treatment, as well as on and off resonance, suggests that hybridization plays a much more important role when examining the Er 4*d* edge, limiting the possibility of obtaining additional information.

However, both results clearly show the additional gain from RES-PES in these Er-filled SWCNT hybrids. The fact that Er is trivalent (e.g., as found from 3*d* XAS or magnetic measurements) is actually very important for the local chemistry, but in order to study the charge distribution in the hybrid compounds by RES-PES it is crucial to understand the detailed changes in their electronic structure. In particular, it is possible to identify the distribution within the Er at the Cl and the hybridization between the Er 5*d* and the carbon $\pi$ orbitals of the SWCNTs. Similar effects have been studied in the case of metallofullerenes for La@$C_{82}$, where La was found to be trivalent with an effective valence of 2.7 and a hybridization of one-third of electron between the La and C (Ref. 27), and Gd@$C_{82}$, where the Gd 4*f* resonance was strongly suppressed as compared to a Gd metal reference.[28] In order to analyze this for the SWCNTs with $ErCl_3$ and Er filling, we explore in detail the resonant photoemission at the 3*d* and 4*d* edges. In this latter situation, we have nanowires and nanoparticles interacting with the nanotubes.

In summary, our RES-PES inspection shows two effects that are in good agreement with the results from XPS and EDX. First, the Cl is lost, which leads to the formation of short encapsulated nanowires and nanoparticles; and secondly, the hybridization to the carbon $\pi$ orbitals is diminished. Therefore, in valence band photoemission, in the latter step, the spectra show a finite charge distribution between the 4*f* and the Er 5*d* orbitals.

## IV. CONCLUSIONS

The possibility of forming elemental rare-earth nanowires templated by SWCNTs is of high technological interest. Quantum $ErCl_3$ nanowires, templated inside carbon nanotubes tailored under high temperature and vacuum, have been studied with a combined XAS and resonant photoemission approach. We have shown here that this occurs spontaneously via thermal heating inside the tubes. The salt filling undergoes a chemical transformation upon high temperature heating in vacuum, leading to the formation of elemental Er nanowires inside the SWCNTs. Although there is a loss of filling, the small nanowires that remain encapsulated in the tubes, as well as the material that diffuses outside the cylindrical structures, is completely transformed into elemental Er. The possible structural models of an encapsulated crystalline $ErCl_3$ nanowire are certainly radically different. Given the diameter distribution in the nonfilled material, and the evidence of a possible 90% filling ratio in unsorted nanotube hollow material, it is possible that a percentage of chiralities and diameters in a bundle of SWCNTs is still able to allow transformation of the $ErCl_3$ and still host elemental Er nanowires. For this reason, a further step definitely involves explaining the Cl loss mechanism to fully understand the formation of elemental Er nanowires inside the SWCNT structure. These filled SWCNTs exhibit a high filling ratio. From XAS and XPS core level spectroscopy of the filler and the SWCNT cage, as well as from RES-PES across the 4*d* and 3*d* edges, the change in the bonding environment and the hybridization upon thermal annealing has been unambiguously proven. This points to an enhanced hybridization for the Er-filled SWCNT, which is in good agreement with the observed lower ionicity of the Er states. This has important implications for addressing the electronic structure in these hybrids by the different interplay between charge transfer and hybridization in metal-filled as well as in salt-filled SWCNTs, and for assessing their application potential in nanochemistry and nanoelectronics.

## ACKNOWLEDGMENTS

This work was supported by the Austrian Science Fund through Project No. FWF P21333-N20 and the German Research Foundation through Project No. DFG PI 440-4/5. H.S. acknowledges the Leverhulme Trust and the EPSRC through a Portfolio Partnership grant. We acknowledge the technical assistance from S. Leger and R. Hübel, from the IFW-Dresden. We acknowledge the Helmholtz-Zentrum Berlin–Electron Storage Ring BESSY II for provision of synchrotron radiation at beamline UE52PGM. The research leading to these results has received funding from the EU (FP7/2007-2013) under Grant Agreement No. 226716. P.A. was supported by the Marie Curie IEF Actions within the 7th European Community Framework Programme.

[1] D. Tomanek, A. Jorio, M. Dresselhaus, and G. Dresselhaus, Carbon Nanotubes **111**, 1 (2008).
[2] P. Ayala, R. Arenal, R. Loiseau, A. Rubio, and A. Pichler, Rev. Mod. Phys. **82**, 1843 (2010).
[3] T. Pichler, H. Kuzmany, H. Kataura, and Y. Achiba, Phys. Rev. Lett. **87**, 267401 (2001).
[4] T. Shimada, T. Okazaki, R. Taniguchi, T. Sugai, H. Shinohara, K. Suenaga, Y. Ohno, S. Mizuno, S. Kishimoto, and T. Mizutani, Appl. Phys. Lett. **81**, 4067 (2002).
[5] S. Bandow, T. Hiraoka, T. Yumura, K. Hirahara, H. Shinohara, and S. Iijima, Chem. Phys. Lett. **384**, 320 (2004).
[6] R. Pfeiffer, T. Pichler, Y. A. Kim, and H. Kuzmany, Carbon Nanotubes **111**, 495 (2008).
[7] R. Kitaura, H. Okimoto, H. Shinohara, T. Nakamura, and H. Osawa, Phys. Rev. B **76**, 172409 (2007).
[8] H. Shiozawa *et al.*, Phys. Rev. B **73**, 075406 (2006).
[9] R. Kitaura, N. Imazu, K. Kobayashi, and H. Shinohara, Nano Lett. **8**, 1530 (2008).
[10] R. Kitaura, D. Ogawa, K. Kobayashi, T. Saito, S. Ohshima, T. Nakamura, H. Yoshikawa, K. Awaga, and H. Shinohara, Nano Res. **1**, 152 (2008).
[11] H. Shiozawa, T. Pichler, A. Gruneis, R. Pfeiffer, H. Kuzmany, Z. Liu, K. Suenaga, and H. Kataura, Adv. Mater. **20**, 1443 (2008).
[12] H. Shiozawa, T. Pichler, C. Kramberger, M. Rummeli, D. Batchelor, Z. Liu, K. Suenaga, H. Kataura, and S. R. P. Silva, Phys. Rev. Lett. **102**, 046804 (2009).

[13]K. H. Hellwege, S. Hufner, and H. G. Kahle, Z. Phys. **160**, 162 (1960).
[14]H. G. Kahle, Z. Phys. **145**, 361 (1956).
[15]G. H. Dieke and S. Singh, J. Chem. Phys. **35**, 555 (1961).
[16]T. Goto, J. Inorg. Nucl. Chem. **30**, 3305 (1968).
[17]E. H. Carlson and H. S. Adams, J. Chem. Phys. **51**, 388 (1969).
[18]T. Saito, W.-C. Xu, S. Ohshima, H. Ago, M. Yumura, and S. Iijima, J. Phys. Chem. B **110**, 5849 (2006).
[19]C. Kramberger, H. Rauf, H. Shiozawa, M. Knupfer, B. Buchner, T. Pichler, D. Batchelor, and H. Kataura, Phys. Rev. B **75**, 235437 (2007).
[20]P. Ayala *et al.*, Phys. Rev. B **80**, 205427 (2009).
[21]P. Ayala, H. Shiozawa, K. De Blauwe, Y. Miyata, R. Follath, H. Kataura, and T. Pichler, J. Mater. Sci. **45**, 5318 (2010).
[22]K. De Blauwe, D. J. Mowbray, Y. Miyata, P. Ayala, H. Shiozawa, A. Rubio, P. Hoffmann, H. Kataura, and T. Pichler, Phys. Rev. B **82**, 125444 (2010).
[23]B. Thole, G. van der Laan, J. Fuggle, G. Sawatzky, R. Karnatak, and J.-M. Esteva, Phys. Rev. B **32**, 5107 (1985).
[24]F. Gerken, J. Phys. F **13**, 703 (1983).
[25]G. van der Laan, B. T. Thole, H. Ogasawara, Y. Seino, and A. Kotani, Phys. Rev. B **46**, 7221 (1992).
[26]D. H. Pearson, C. C. Ahn, and B. Fultz, Phys. Rev. B **47**, 8471 (1993).
[27]B. Kessler, A. Bringer, S. Cramm, C. Schlebusch, W. Eberhardt, S. Suzuki, Y. Achiba, F. Esch, M. Barnaba, and D. Cocco, Phys. Rev. Lett. **79**, 2289 (1997).
[28]M. S. Golden, T. Pichler, and P. Rudolf, in *Fullerene-Based Materials: Structures and Properties*, edited by Kosmas Prassides (Springer-Verlag, Berlin Heidelberg, 2004), Vol. 109, p. 201.